



THE UNIVERSITY *of* EDINBURGH

## Edinburgh Research Explorer

# Effect of (quasi-)optimum model parameter sets and model characteristics on future discharge projection of two basins from Europe and Asia

### Citation for published version:

Chamorro, A, Kraft, P, Pauer, G, Exbrayat, J-F & Breuer, L 2017, 'Effect of (quasi-)optimum model parameter sets and model characteristics on future discharge projection of two basins from Europe and Asia' *Climatic Change*, vol 142, no. 3, pp. pp 559–573. DOI: 10.1007/s10584-017-1974-4

### Digital Object Identifier (DOI):

[10.1007/s10584-017-1974-4](https://doi.org/10.1007/s10584-017-1974-4)

### Link:

[Link to publication record in Edinburgh Research Explorer](#)

### Document Version:

Peer reviewed version

### Published In:

*Climatic Change*

### Publisher Rights Statement:

© Springer Science+Business Media Dordrecht 2017

### General rights

Copyright for the publications made accessible via the Edinburgh Research Explorer is retained by the author(s) and / or other copyright owners and it is a condition of accessing these publications that users recognise and abide by the legal requirements associated with these rights.

### Take down policy

The University of Edinburgh has made every reasonable effort to ensure that Edinburgh Research Explorer content complies with UK legislation. If you believe that the public display of this file breaches copyright please contact [openaccess@ed.ac.uk](mailto:openaccess@ed.ac.uk) providing details, and we will remove access to the work immediately and investigate your claim.



# Climatic Change

## Effect of (quasi-)optimum model parameter sets and model characteristics on future discharge projection of two basins from Europe and Asia

--Manuscript Draft--

<b>Manuscript Number:</b>	
<b>Full Title:</b>	Effect of (quasi-)optimum model parameter sets and model characteristics on future discharge projection of two basins from Europe and Asia
<b>Article Type:</b>	Research Article
<b>Corresponding Author:</b>	Alejandro Chamorro Chavez, Dr Justus Liebig University Giessen Giessen, GERMANY
<b>Corresponding Author Secondary Information:</b>	
<b>Corresponding Author's Institution:</b>	Justus Liebig University Giessen
<b>Corresponding Author's Secondary Institution:</b>	
<b>First Author:</b>	Alejandro Chamorro Chavez, Dr
<b>First Author Secondary Information:</b>	
<b>Order of Authors:</b>	Alejandro Chamorro Chavez, Dr Philipp Kraft Gesa Pauer Jean-Francois Exbrayat Lutz Breuer
<b>Order of Authors Secondary Information:</b>	
<b>Funding Information:</b>	
<b>Abstract:</b>	<p>Uncertainty is an inherent, unavoidable feature in the modeling of natural processes. This is particularly a sensitive issue when dealing with forecasting, especially in the context of climate change impacts. Apart from the uncertainty introduced by different climate projections, additional sources of uncertainty appear in the analysis of rainfall-runoff and associated prediction of water discharge changes due to climate change models, input information in calibration steps, regionalization, parameter choices, and downscaling techniques, among others. In this study, we focus on the uncertainty introduced by various set of parameters in the 21st century projections of runoff for two large river basins: the Rhine river in Europe, and the Ganges in Asia. To estimate the relative impact of parameter-induced uncertainty, various scenarios are compared with those given by general circulation models (GCM) and climate change emission scenarios (Representative Concentration Pathways, RCP). We apply a robust parameter estimation optimization algorithm ROPE to account for the uncertainty in a quasi-optimum parameter set choice. A total of 1,000 well performed parameter sets are analyzed for this purpose. Also, two hydrological models are used to test the impact of model conception. The analysis of the ensemble of projected discharge suggests that the parameter uncertainty is strongly related to model complexity in both basins considering the best one thousand performing sets. The contribution to uncertainty of parameter sets for the Ganges is rather stable in time and comparatively small for the periods 2006 to 2035, 2036 to 2065 and 2070 to 2099. Major differences are attributable to GCMs ranging from 60% to 80% followed by RCPs in the range 12-30%, whereas parameter differences account for 3-8%. Results for the Rhine are more heterogeneous and change over time, with increasing importance of GCM/RCPs toward the end of the century. The major differences are also observed in the GCM outcomes representing a proportion of 49-77% in contrast to 11-40% of model parametrization (parameter sets).</p>

<b>Suggested Reviewers:</b>	Chandana gangodagamage, Dr NOAA Chandana.gangodagamage@noaa.gov
	Shailesh Singh, Dr National Institute of Water and Atmospheric Research Christchurch Office shailesh.singh@niwa.co.nz
	Jens Goetzinger, Dr Ministerium fuer Umwelt, Energie und Verkehr, Saarbruecken j.goetzinger@umwelt.saarland.de
	Waldo Lavado, Dr National Service of Meteorology and Hydrology, Peru directorioctei@conytec.gob.pe

[Click here to view linked References](#)

1  
2  
3  
4  
5  
6  
7  
8  
9  
10  
11  
12  
13  
14  
15  
16  
17  
18  
19  
20  
21  
22  
23  
24  
25  
26  
27  
28  
29  
30  
31  
32  
33  
34  
35  
36  
37  
38  
39  
40  
41  
42  
43  
44  
45  
46  
47  
48  
49  
50  
51  
52  
53  
54  
55  
56  
57  
58  
59  
60  
61  
62  
63  
64  
65

1  
2  
3  
4 2  
5  
6  
7 3 **Effect of (quasi-)optimum model parameter sets and model characteristics on future**  
8  
9 4 **discharge projection of two basins from Europe and Asia**

10  
11 5  
12  
13 6 **A. Chamorro, P. Kraft, G. Pauer, J.-F. Exbrayat, L. Breuer**

14  
15 7  
16  
17 8 date of receipt and acceptance should be inserted later

19 9  
20  
21 10 **Abstract**

22  
23 11 Uncertainty is an inherent, unavoidable feature in the modeling of natural processes. This is particularly a  
24 12 sensitive issue when dealing with forecasting, especially in the context of climate change impacts. Apart from  
25 13 the uncertainty introduced by different climate projections, additional sources of uncertainty appear in the  
26 14 analysis of rainfall-runoff and associated prediction of water discharge changes due to climate change models,  
27 15 input information in calibration steps, regionalization, parameter choices, and downscaling techniques, among  
28 16 others. In this study, we focus on the uncertainty introduced by various set of parameters in the 21<sup>st</sup> century  
29 17 projections of runoff for two large river basins: the Rhine river in Europe, and the Ganges in Asia. To estimate  
30 18 the relative impact of parameter-induced uncertainty, various scenarios are compared with those given by  
31 19 general circulation models (GCM) and climate change emission scenarios (Representative Concentration  
32 20 Pathways, RCP). We apply a robust parameter estimation optimization algorithm ROPE to account for the  
33 21 uncertainty in a quasi-optimum parameter set choice. A total of 1,000 well performed parameter sets are  
34 22 analyzed for this purpose. Also, two hydrological models are used to test the impact of model conception. The  
35 23 analysis of the ensemble of projected discharge suggests that the parameter uncertainty is strongly related to  
36 24 model complexity in both basins considering the best one thousand performing sets. The contribution to  
37 25 uncertainty of parameter sets for the Ganges is rather stable in time and comparatively small for the periods  
38 26 2006 to 2035, 2036 to 2065 and 2070 to 2099. Major differences are attributable to GCMs ranging from 60%  
39 27 to 80% followed by RCPs in the range 12-30%, whereas parameter differences account for 3-8%. Results for  
40 28 the Rhine are more heterogeneous and change over time, with increasing importance of GCM/RCPs toward  
41 29 the end of the century. The major differences are also observed in the GCM outcomes representing a proportion  
42 30 of 49-77% in contrast to 11-40% of model parametrization (parameter sets).

53  
54 31  
55  
56 32  
57  
58 33 

---

A. Chamorro, P. Kraft, P. Gesa

59  
60 34 Institute of Landscape Ecology, Justus Liebig University, Giessen, Germany

1 35 E-mail: alejandro.chamorro-chavez@umwelt.uni-giessen.de

2  
3 36

4  
5 37 J.-F. Exbrayat

6  
7 38 School of GeoSciences and National Centre for Earth Observation, University of Edinburgh,

8  
9 39 Edinburgh, UK

10  
11 40

12  
13 41 L. Breuer

14  
15 42 Centre for International Development and Environmental Research Justus Liebig University Giessen.

16  
17 43 Institute of Landscape Ecology, Justus Liebig University, Giessen, Germany

18  
19 44

20  
21 45 **Keywords:** Depth function, ROPE algorithm, uncertainty analysis, Climate change impact, Rhine river, Ganges

22  
23 46 river, rainfall-runoff modelling

24  
25 47

## 26 27 48 **1. Introduction**

28  
29 49  
30  
31 50 Mathematical representation and state representation at a given time of a natural phenomenon that allow a precise

32  
33 51 description and detailed picture of the phenomenon is not possible. In the context of hydrological modelling,

34  
35 52 several sources of errors and uncertainties have been identified. Although there are various classifications, the

36  
37 53 main sources of predictive uncertainty can be divided according to input uncertainty, state uncertainty, process

38  
39 54 abstraction-related uncertainty, model structure uncertainty and output uncertainty (Götzinger and Bárdossy,

40  
41 55 2008). In spite of their role, addressing their relative contribution to the final predictive uncertainty is far from

42  
43 56 being trivial. Furthermore, predictive uncertainty is often partially assessed as the best model state, evaluated with

44  
45 57 defined goodness-of-fit metrics (Singh and Woolhiser, 2002). Isolating source of errors and quantifying their

46  
47 58 contribution to the overall predictive uncertainty has been matter of various efforts (Kavetski et al., 2003; Schaepli

48  
49 59 et al., 2007). This can be significant when future statements are pursued, and a certain confidence is expected.

50  
51 60 Several researchers have investigated uncertainty for climate change projections. Efforts have been placed in

52  
53 61 various aspects including input data uncertainties in the process of calibration and validation, downscaling related

54  
55 62 uncertainties, general circulation models (GCMs) and rainfall-runoff models, among others. The object of analysis

56  
57 63 can affect the impact on mean discharge values, flood frequency, extreme values or drought characteristics. Teng

58  
59 64 et al., 2011 for example assessed the relative uncertainties in modeling climate change impact on runoff across

60  
61  
62  
63  
64  
65

1 65 southeast Australia given by GCMs and rainfall-runoff models. Their results showed that uncertainty sourced from  
2  
3 66 the GCMs is much larger than the uncertainty in the rainfall-runoff models. The contribution of various sources of  
4  
5 67 uncertainty have also been investigated by Exbrayat et al., 2014 for a remote and data-sparse catchment in Ecuador.  
6  
7 68 There, the contribution of differences between model structures to the total uncertainty was found to be similar  
8  
9 69 compared to GCM and emission scenarios for discharge simulations. Harding et al., 2012 investigated the impact  
10  
11 70 of future climate conditions using a multi-model ensemble approach from 16 GCMs in the Upper Colorado River  
12  
13 71 Basin. They found that the impact of projected 21th century climate conditions on streamflow ranges from a  
14  
15 72 decrease of approximately 30% to an increase of similar magnitude. Jung and Chang, 2011 studied runoff trends  
16  
17 73 under multiple climate change scenarios consisting of 8 GCMs and 2 emission scenarios, and the effects of  
18  
19 74 elevation and geological characteristics on uncertainty. Some of their results showed that long-term trends of water  
20  
21 75 balance components in the Willamette River Basin can be highly affected by anthropogenic climate change.  
22  
23 76 The parameter uncertainty has been a topical subject in rainfall-runoff modeling in the last decades (Beven and  
24  
25 77 Binley, 1992), especially in the context of climate change. For example, Wilby, 2005, analyzed the uncertainty  
26  
27 78 related to model parameter for climate change impact assessments in the River Thames, UK. He explored the  
28  
29 79 effect of the non-uniqueness of parameters on projections using hydrological model CATCHMOD. Uncertainty in  
30  
31 80 future river flows was explored using the 100 best performing parameter sets generated by Monte Carlo simulation.  
32  
33 81 Wilby and Harris, 2006, presented a probabilistic approach for combining sources of uncertainties such as emission  
34  
35 82 scenario, GCM, downscaling techniques, parameter model parameters and model structure for the River Thames  
36  
37 83 and low-flow scenarios. Uncertainty due to parameter choice was addressed by using two sets and found that low-  
38  
39 84 flow cumulative distribution functions are most sensitive to uncertainty in the climate change scenarios and  
40  
41 85 downscaling of different GCMs.  
42  
43 86 Overall, quantification of uncertainty has been a major topic in hydrology, where substantial effort have been  
44  
45 87 placed into their effects in climate change scenarios. The contribution of the different uncertainty sources or the  
46  
47 88 main sources remains as an outstanding open problem, where case-dependent characterization appears be the most  
48  
49 89 appropriate approach. Addressing all potential uncertainty sources is far from the scope of most or possibly all  
50  
51 90 research studies we can find in the literature.  
52  
53 91 While the major uncertainty sources have been attributed to GCMs in the aforementioned studies, other  
54  
55 92 investigations have arrived to different conclusions. For example, Haddeland et al., 2011 used a multimodel  
56  
57 93 approach for models intercomparison and showed that major source of uncertainty are due to considerable  
58  
59 94 differences in simulated runoff between models. They pointed that studies of climate change impacts should not  
60  
61  
62  
63  
64  
65

1 95 be based on a single model. Nonetheless, Uncertainty in rainfall-runoff modeling can be caused by both model  
2  
3 96 structure and parameters (Teng et al., 2011).

4  
5 97 In this study, we investigate the effect of various sets of parameters on the projected discharge of Rhine at Lobith  
6  
7 98 located in Europe and Ganges at Farakka located in Asia for the periods 2006-2035, 2036-2065, and 2070-2099.  
8  
9 99 We apply a robust parameter optimization algorithm (ROPE) to generate a large number ( $n=1,000$ ) of well  
10  
11 100 performing parameter sets for each instance. We address the influence of model structures/complexity on these  
12  
13 101 projections by using two state-of-the-art hydrological models. First, we calibrate and validate against observed  
14  
15 102 discharge. Then, we use climate projections from five GCMs driven by four Representative Concentration  
16  
17 103 Pathways (RCPs) emission scenarios for the 21<sup>st</sup> century. GCMs chosen here present ranges of uncertainties in  
18  
19 104 projections of annual temperature and precipitation comparable with all of CMIP5 models (see protocol-report on  
20  
21 105 [www.isimip.org](http://www.isimip.org)).

## 27 108 2. Material and methods

### 29 109 31 110 2.1 Study areas and available data

33 111  
34  
35 112 Main features of the Rhine River at Lobith's and the Ganges at Farakka's basins can be found in the introductory  
36  
37 113 paper of the Inter-Sectoral Impact Model Intercomparison Project Phase 2 ISI-MIP2 (Krysanova and Hattermann,  
38  
39 114 2016). The WATCH forcing dataset is used to calibrate and validate the hydrological models. It is based on the  
40  
41 115 40-yr ECMWF Re-Analysis (ERA-40) and reordered reanalysis data for 1958-2001 and 1901-1951, respectively.  
42  
43 116 The dataset contain several climatological variables including air temperature, rainfall rate, specific humidity,  
44  
45 117 amongst others, which are regularly distributed grids with 0.5 degree resolution. For details on WATCH and ERA-  
46  
47 118 40 refer to Weedon et al., 2011 and Uppala et al., 2005.

49 119 Climate change scenario data are based on five GCMs participating in the Coupled Model Intercomparison Project  
50  
51 120 Phase 5 (Taylor et al., 2012): HadGEM2-ES, IPSL CM5A-LR, MIROC-ESM-CHEM, GFDL-ESM2M, and  
52  
53 121 NorESM1-M. These models are based on a set of different scenarios accounting for anthropogenic fossil-fuel  
54  
55 122 emissions as well as land use and land cover change. We use 20 combinations consisting of five GCMs and four  
56  
57 123 representative concentration pathways (RCP2.6, RCP4.5, RCP6.0 and RCP8.5) scenarios; last identified by the  
58  
59 124 approximate gain in radiative forcing in year 2100 mostly due to human emissions of greenhouse gases compared  
60  
61  
62  
63  
64  
65

1 125 to the baseline level in 1750 (IPCC 2013). These climate projections were downscaled and bias corrected following  
2  
3 126 Hempel et al., 2013.

4  
5 127

6  
7 128

## 8 9 129 2.2 Hydrological models

10  
11 130

12  
13 131 Parameter values affect the outcomes of a model. This may induce not negligible variations of the simulated  
14  
15 132 discharges. In order to account for this effect, two conceptual hydrological models, namely HBV and HYMOD  
16  
17 133 are used to evaluate this interdependence. A large number of robust parameter sets (see section 2.3) is search for  
18  
19 134 and the variations in the simulations is compared for each model.

20  
21 135 The semi-distributed HVB model is a rainfall-runoff type originally developed by the Swedish Meteorological  
22  
23 136 and Hydrological Institute (SMHI) (Bergström, 1995; Lindström et al., 1997). This conceptually based model  
24  
25 137 comprises routines for calculating snow accumulation and melt, soil moisture, and runoff generation as a function  
26  
27 138 of soil water content and infiltration rates, runoff concentration and discharge flood routing within the river  
28  
29 139 network. Our HBV version uses modified components; for example, the incorporation of a new parameter in the  
30  
31 140 degree-day factor for accounting additional energy available in rainwater at positive temperatures, and a non-  
32  
33 141 linearity of the rainfall-runoff proportion expressed by a power-law relationship. Details can be found in Hundecha  
34  
35 142 and Bárdossy, 2004, and Hundecha Hirpa, 2005.

36  
37 143 The HYMOD is a relatively simpler conceptual rainfall-runoff model defined by two components, namely the  
38  
39 144 rainfall excess (two parameters) and two series of linear reservoirs (three parameters) arranged in parallel. The  
40  
41 145 first reservoir represents a quick response and the second one a slow response. The version used here also considers  
42  
43 146 a snow routing routine as in the HBV model. Details can be found in Moore, 1985, Boyle et al., 2001 and Wagener  
44  
45 147 et al., 2001.

46  
47 148

48  
49 149

## 50 51 150 2.3 Robust Parameter Estimation

52  
53 151

54  
55  
56 152 Robust Parameter Estimation (ROPE) optimization procedure is performed to get an estimation of the uncertainty  
57  
58 153 in the expected discharge variation due to parameter choice. The analysis of geometrical properties of parameter  
59  
60 154 sets is key. It has been investigated by Bárdossy, 2007 in a 2D case showing a well-defined structure of the sets.

61  
62  
63  
64  
65



1 155 Later, Bárdossy and Singh, 2008, Singh, 2010, investigated these properties in a hydrological modeling framework  
 2  
 3 156 in higher dimensions. The parameter search aims to find robust sets that have important features such as good  
 4  
 5 157 model performance in the selected period, a reasonable representation of the modelled processes, small sensitivity  
 6  
 7 158 and transferability to other time periods. This was investigated in detail by Bárdossy and Singh, 2008. However,  
 8  
 9 159 to the best of our knowledge a robust parameter estimation has not been performed to generate an ensemble of  
 10  
 11 160 well-performing parameter sets in the scope of climate change uncertainty assessment. Hereafter, we briefly  
 12  
 13 161 describe the ROPE algorithm and the underlying calculations of parameter depth, the key concept in the search of  
 14  
 15 162 optimum parameter sets.

### 165 Depth function

166  
 167 The depth function was first introduced by Tukey, 1975, as a measure of centrality of a data set within a population  
 168 set in a multi-dimensional space. Let  $\mathbf{x}$  be a vector from a set  $S$  such that  $\mathbf{x} \in S$ , and  $S \subseteq R^p$ . A depth function is  
 169 defined as:

$$D: R^p \rightarrow R$$

$$\{\mathbf{x} \in R^p\} \rightarrow y$$

170  
 171 in which to each vector  $\mathbf{x}$ , a number (depth)  $y$  is associated so that an ordering of  $\mathbf{x} \in S$  in the center-outward  
 172 direction is defined. It can be seen as a quantitative measure of how central a vector is located when compared  
 173 with a given vector set. Several definitions of depth function have been proposed; for example, Liu, 1990 indicated  
 174 non-negativeness and a bounded domain as a prerequisite to be fulfilled. Others include Affine invariance,  
 175 maximality at center, monotonicity relative to deepest point and vanishing at infinite (Zuo and Serfling, 2000).  
 176 From the listed properties follow that the data lying in the vicinity of the center of the cloud have a high depth  
 177 value; conversely, those located far from the center have a low depth value. More details can be found in Donoho  
 178 and Gasko, 1992, Miller et al., 2003. Others depth functions include the  $L_1$  depth ((Hugg et al., 2006), Oja median  
 179 (Oja, 1983), Convex Hull Peeling (Barnett, 1976; Liu et al., 1999), Likelihood-based depth functions (Fraiman et  
 180 al., 1997) and a method for constructing individual depth functions (Vardi and Zhang, 2000).

### 184 Halfspace depth function

1 185  
 2  
 3 186 Tukey, 1975, proposed the halfspace depth function as a kind of generalization in the multivariate space of the  
 4  
 5 187 univariate rank (order statistics). The depth of a point  $\mathbf{p} = \{p_i\}_{i=1}^d$  in dimensional space  $d$  with respect to a finite  
 6  
 7 188 set  $\mathbf{X}$  is defined as the minimum number of points in  $\mathbf{X}$  lying on one side of a hyperplane though the point  $\mathbf{p}$ .  
 8  
 9 189 Considering all possible directions for the hyperplane given by its unit normal vector the minimum is then  
 10  
 11 190 calculated, and mathematically expressed as:

$$12$$

$$13$$

$$14$$

$$15$$

$$16$$

$$17$$

$$18$$

$$19$$

$$20$$

$$21$$

$$22$$

$$23$$

$$24$$

$$25$$

$$26$$

$$27$$

$$28$$

$$29$$

$$30$$

$$31$$

$$32$$

$$33$$

$$34$$

$$35$$

$$36$$

$$37$$

$$38$$

$$39$$

$$40$$

$$41$$

$$42$$

$$43$$

$$44$$

$$45$$

$$46$$

$$47$$

$$48$$

$$49$$

$$50$$

$$51$$

$$52$$

$$53$$

$$54$$

$$55$$

$$56$$

$$57$$

$$58$$

$$59$$

$$60$$

$$61$$

$$62$$

$$63$$

$$64$$

$$65$$

$$D_x(\mathbf{p}) = \min_{\mathbf{n}_h} (\min(|\{\mathbf{x} \in \mathbf{X}, \langle \mathbf{n}_h, \mathbf{x} - \mathbf{p} \rangle > 0\}|), (|\{\mathbf{x} \in \mathbf{X}, \langle \mathbf{n}_h, \mathbf{x} - \mathbf{p} \rangle < 0\}|)) \quad (1)$$

193  
 194 In this equation  $\langle \boldsymbol{\alpha}, \boldsymbol{\beta} \rangle$  and  $\mathbf{n}_h$  represent the scalar product and an arbitrary unit vector of a selected hyperplane so  
 195 that  $\mathbf{n}_h \in R^d$ . The dimension of the space is denoted by  $d$ . The scalar product represents the projection of the  
 196 vector  $(\mathbf{x} - \mathbf{p})$  onto the unit vector  $\mathbf{n}_h$ . It can be shown that this depth function satisfies all properties listed in the  
 197 previous point (Zuo and Serfling, 2000). In this study, the calculation of the depth is based on that suggested by  
 198 Rousseeuw and Struyf, 1998, which is an approximate estimation of the location depth, especially appropriate  
 199 when dealing with large data sets or a high-dimension parameter space (number of parameters).

200  
 201  
 202 ROPE algorithm

203  
 204 As suggested by Bárdossy and Singh, 2008, the following optimization procedure is used to find a set of good  
 205 performing and deep parameter vectors for robustness in the modelling step. Given the dimension of the parameter  
 206 vector  $d$ ,

- 207
- 208 1. Identify the limits for the  $d$  selected parameters.
- 209 2. Generate  $n$  random parameter vectors conforming the set  $\mathbf{X}_n = \{\boldsymbol{\theta}_1, \dots, \boldsymbol{\theta}_n\}$ ,  $\boldsymbol{\theta}_j \in R^d$ ,  $j = 1, \dots, n$ . The  
 210 limits are those defined in 1
- 211 3. Run the hydrological model For each parameter vector  $\boldsymbol{\theta}_i \in \mathbf{X}_n$ , and calculate the performances of the  
 212 model  $\{g_{\theta_i}\}_{i=1}^n$ .
- 213 4. Define a new set  $\mathbf{X}_m$  containing the  $m$ -parameter vectors with the best performance. The number of the  
 214  $m$  selected vectors can be for example the 10% of best performing vectors from  $\mathbf{X}_n$ .

1 215 5. Generate a set of  $p$  new random vectors  $\mathbf{Y}_p$  such that

$$2 \mathbf{Y}_p = \{\boldsymbol{\theta}_1, \dots, \boldsymbol{\theta}_p / D(\boldsymbol{\theta}_i) \geq L, i = 1, \dots, p\}$$

3 216  
4  
5 217 In this step, the depth  $D(\boldsymbol{\theta})$  is calculated with respect to the set  $\mathbf{X}_m$  defined in the previous step.

6  
7 218 6. Relabel the constructed vector set  $\mathbf{Y}_p$  as  $\mathbf{X}_n$  and repeat the procedure from point 3

8  
9 219  
10  
11 220 As expected, for increased number of iterations in step 3, the run time involved in each step also increases.  
12  
13 221 Consequently, the algorithm can be stopped when the performance of two consecutive simulation steps does not  
14  
15 222 differ more than expected from the observation errors (Bárdossy and Singh, 2008). Note that it depends on specific  
16  
17 223 factors such as the amount of data (range of the period used for calibration and validation); the entire process may  
18  
19 224 be computationally expensive. Here, the performance of the parameters plays also an important role in the required  
20  
21 225 iterations.

## 22 226 23 24 227 25 26 228 2.4 Experimental setup

27  
28 229  
29  
30 230 Uncertainty in model projections due to good performing robust parameter vectors is based on the  $n_{opt} = 1000$   
31  
32 231 parameters from the last iteration of ROPE showing the best performance. The commonly-used Nash-Sutcliffe  
33  
34 232 function was chosen (Nash and Sutcliffe, 1970) as objective function for model evaluation. The initial number of  
35  
36 233 parameter vectors randomly generated is set to  $n_0 = 100,000$ ; each parameter having plausible lower and upper  
37  
38 234 limits previously defined. The number of best performing parameter vectors after running the model is set to  $m =$   
39  
40 235 1,000. Finally  $n_p = 5,000$  number of vectors are generated in each iteration through Monte Carlo Simulations  
41  
42 236 constrained to  $depth > 1$  (eq.1). Parameter related uncertainty is calculated based on the range of projected discharge  
43  
44 237 out of this final set.

45  
46 238 As pointed, the effect on this uncertainty due to model structure is analyzed comparing the hydrologic simulation  
47  
48 239 given by the two hydrological models HBV and HYMOD. Effects of GCMs and RCPs on the parameter  
49  
50 240 uncertainty are also included in this analysis. An ensemble of simulations is performed for each basin considering  
51  
52 241 one GCM and one RCP. A set of 20 combinations is compared for HBV and HYMOD, and for the two basins  
53  
54 242 Rhine and Ganges. Finally, we summarize the relative contribution of parameter sets, rainfall-runoff model and  
55  
56 243 GCM choice to the overall uncertainty.

57 244

58  
59  
60  
61  
62  
63  
64  
65

1 245  
2  
3 246 **3 Results and discussion**  
4

5 247  
6  
7 248 3.1 Optimization results  
8

9 249  
10  
11 250 An iteration traduces in a set of better performing parameter sets. This can be easily observed by comparing the  
12  
13 251 distribution of the set performance step by step. Figure 1 shows the histograms for the two models HBV and  
14  
15 252 HYMOD and for the two basins, Rhine and Ganges. Each histogram is built out of 5,000 parameter sets generated  
16  
17 253 so that  $depth > 1$  (eq. 1). The subplots include the histograms of three consecutive iterations showing the evolution  
18  
19 254 of the parameter set performance. It is observed that the mean value as well as the spread in each iteration varies  
20  
21 255 significantly. The range for the objective function evaluation corresponding to the last iteration involving selected  
22  
23 256 best  $n_{opt} = 1,000$  vectors used for simulations varies from  $NS = 0.845$  to  $NS = 0.867$  for HBV and from  $NS =$   
24  
25 257  $0.70$  to  $NS = 0.79$  for HYMOD. Performances show a larger spread for the Rhine basin from standard deviation  
26  
27 258  $std = 0.012$  to  $std = 0.016$  in contrast to Ganges with limits  $std = 0.004$  and  $std = 0.006$ . Statistics as the  
28  
29 259 mean, minimum and maximum values for the best  $n=1000$  performing final sets are summarized in table 1.  
30

31 260  
32  
33 261  
34  
35 262 3.2 Parameter related uncertainty in future projections  
36

37 263  
38  
39 264 The prime focus of this study is on the quantification parameter uncertainty has in future discharge projections. A  
40  
41 265 large number ( $n=1,000$ ) well performing parameter sets derived from the last iteration of ROPE are used to draw  
42  
43 266 the range/uncertainty out of all possible simulated discharge for each basin and model. We consider the 90%  
44  
45 267 confidence interval of the simulated discharge curves for the three defined time periods.  
46  
47

48 268 The analysis reveals differences depending on the model used and region under consideration. When comparing  
49  
50 269 parameter uncertainty contrasting HBV and HYMOD, uncertainty associated to HBV is smaller than that observed  
51  
52 270 by HYMOD in terms of the mean values. This occurs in both the Rhine and the Ganges basins. While HBV shows  
53  
54 271 expected uncertainties of  $d = 4.67\%$  and  $d = 1.69\%$  for Rhine and Ganges respectively, HYMOD present  
55  
56 272 uncertainties of  $d = 5.389\%$  and  $d = 6.921\%$ . Analyzing results given by HBV model, uncertainty might be  
57  
58 273 considered not significant when compared with differences given by other sources such as GCMs. This is clear in  
59  
60 274 the case of Ganges in which parameter associated uncertainty shows a significant smaller mean value in the  
61  
62  
63  
64  
65

1 275 projection range (about 1/3 of that corresponding to Rhine with a magnitude of 1.69% in the complete period).  
2  
3 276 The simpler model HYMOD shows more uncertainty attributed to parameter choice in both analyzed regions,  
4  
5 277 although the difference between them is not as accentuated as for HBV in terms of mean values. This suggests the  
6  
7 278 effect that model structures have on the expected parameter related uncertainties: A more-complex structure yield  
8  
9 279 to a smaller uncertainty estimation. Same conclusion has been pointed in others studies from other regions. Wilby,  
10  
11 280 2005, found that uncertainty in projected river flows changes in Thames basin, UK was more significant in simpler  
12  
13 281 model structures (comparable to emission scenarios uncertainties) than those from more-complex model  
14  
15 282 structures. The analysis was based on Monte Carlo simulations by randomly generating parameter values, and  
16  
17 283 considering the best 100 performing sets for analysis. Considering two sets of hydrological models parameters,  
18  
19 284 Wilby and Harris, 2006, analyzed Low-flow scenarios for the River Thames and found the uncertainties less  
20  
21 285 important than those given by GCMs.  
22  
23 286 The difference in the projected uncertainties has impacts on the contribution to the total uncertainty, as showed in  
24  
25 287 the next section. Inter-period comparisons considering one RCP separately also present differences, but in general  
26  
27 288 (with some exceptions, e.g. RCP8.5 and period 2006-2035) they do not exhibit important differences. Figure 2  
28  
29 289 shows the associated parameter related uncertainties for both impact models and the two regions in the whole  
30  
31 290 period of analysis (2006-2099). It can be shown that the time periods present similar behavior. Each case consider  
32  
33 291  $n=1,000$  well-performing parameter sets found in the optimization step. Each boxplot summarize the calculated  
34  
35 292 uncertainties for each of the five GCMs and four RCPs comprising a set of 20 points. Each point of each boxplot  
36  
37 293 refers to the uncertainty out of 1000 parameter sets for a certain and single GCM and RCP.  
38  
39  
40  
41  
42

### 43 296 3.3 Quantifying the contribution of hydrological models and GCMs to future projection discrepancies

44  
45  
46

47 298 It is acknowledged that GCMs may have a major impact on the projections relative to other sources; for example  
48  
49 299 rainfall-runoff models in different environments. Teng et al., 2011 showed this in a dry condition, while Chen et  
50  
51 300 al., 2011, in a snow-dominated area. Recently, Exbrayat et al., 2014, analyzed the uncertainty given by seven  
52  
53 301 hydrological models in terms of the relative contribution to the total range of projections. In a context with limited  
54  
55 302 historical calibration data, they found that differences in projections given by different hydrological model  
56  
57 303 structures may be comparable to GCMs for two SRES scenarios in the near-future. Also, the climate projections  
58  
59 304 uncertainties grew toward the end of the 21<sup>st</sup> century. Although we use less ( $n = 5$ ) GCMs compared to Exbrayat  
60  
61  
62  
63  
64  
65

1 305 et al. (2014), it is observed that they nevertheless dominate the differences in projections in the context of our  
2  
3 306 study, as shown in Figures 3 and 4.

4  
5 307 Here, we analyze the spread of the differences in projections out of GCMs choice and two hydrological models,  
6  
7 308 and calculate the relative contribution of hydrological models and GCMs to the overall range in the projections.  
8  
9 309 Projections are calculated by means of a single optimum parameter set calculated for each GCM and hydrological  
10  
11 310 model, as a part of the Inter-Sectoral Impact Model Intercomparison Project Phase 2 ISI-MIP2 (Krysanova and  
12  
13 311 Hattermann, 2016). We also consider the previously defined five GCMs, the four RCPs as well as the three  
14  
15 312 defined periods independently to disaggregate the effects. Uncertainty given by model parametrization is included  
16  
17 313 in the final results to provide a general view.

18  
19 314 As expected, results indicate that the major contribution to differences is given by GCMs independently of the  
20  
21 315 RCP and period under consideration. This has been suggested by several authors in the analysis of different  
22  
23 316 regions. Using a multi-model ensemble consisting of 112 future climate projections from 16 GCMs, Harding et  
24  
25 317 al., 2012 showed that the effect of different scenarios on projected streamflow changes is small relative to the  
26  
27 318 effect of GCMs in the Upper Colorado River Basin. However, our study suggests that this relative contribution is  
28  
29 319 case dependent. The projection divergences for the Rhine river, with exception of the first period of RCP4.5 and  
30  
31 320 RCP8.5, is largely explained by GCMs, with a minimum of round 50%. For the Ganges, the minimum value  
32  
33 321 (contribution) is roughly 70%, which indicates that GCMs explain divergences in large part for both regions. The  
34  
35 322 maximum expected differences do not differ significantly with each other; they are 78.1% and to 83.9% for the  
36  
37 323 Rhine and Ganges. These results are in agreement when considering the expected uncertainty contribution as a  
38  
39 324 function of time (period), which occurs in the mid-century (2036-2065) in both regions. The dependency  
40  
41 325 difference-Region found here has also been acknowledged by other authors. E.g., Based on the analysis on three  
42  
43 326 basins with different elevation and geology characteristics in the Willamette River Basin, USA, Jung and Chang,  
44  
45 327 2011 found that apart from the more significant contribution of GCMs the uncertainty differences depend on the  
46  
47 328 catchment under study.

49 329 The relative contribution of model impacts obtained from the parameter sets is found smaller than those given by  
50  
51 330 GCMs. Projected discharge time series analysis show that HBV estimates slightly higher discharge values  
52  
53 331 compared to HYMOD. Same pattern is shown irrespective of the chosen GCM. HBV present a smaller uncertainty  
54  
55 332 in projections, which is in agreement with the results previously highlighted. As mentioned, this is a general result  
56  
57 333 independent of the time period and model (GCM). To visualize how model impacts may influence the uncertainty  
58  
59 334 given by parameter selection, plots of projected discharge contrasting the two rainfall-runoff models are shown in  
60  
61  
62  
63  
64  
65

1 335 figure 5 as cumulative runoff. As pointed earlier, other time periods and models show similar patterns and, hence,  
2  
3 336 are not shown here for brevity.

4  
5 337 Exploring both regions, differences in the discharge projections for the Ganges are mainly driven by GCMs and  
6  
7 338 models impacts. In contrast, the Rhine shows a different pattern that balances impact models effect and parameter  
8  
9 339 sets uncertainty, which become even more significant in the period 2006-2035 (disregarding GCMs). Figures 3  
10  
11 340 illustrates the results for each RCP and time period for the basin Ganges at Farakka, whereas figure 4 summarizes  
12  
13 341 the same results for Rhine basin at Lobith. The GCMs induces the major differences in projections; parameter  
14  
15 342 uncertainty contribute to a less extent, but it may become comparable to the RCPs differences.

#### 17 343 18 19 344 20 21 345 **4 Conclusions**

22  
23 346  
24  
25 347 This study focused on the analysis and characterization of model parameterization uncertainty and the effect on  
26  
27 348 this uncertainty given by different GCMs ( $n=5$ ), RCPs ( $n=4$ ) and impact models ( $n=2$ ). For this purpose, ensemble  
28  
29 349 of simulated discharge projections were compared for three future periods. The analysis was carried out in two  
30  
31 350 basins from Europe and Asia. Expected parameter uncertainty was estimated performing the ROPE algorithm  
32  
33 351 which is based on the half-space depth function to produce robust parameter sets. In each step  $n=5,000$  sets were  
34  
35 352 generated such that  $depth \geq 1$  and found  $n=1,000$  well performing parameter sets. These quasi-optimum sets  
36  
37 353 were then used to run the models under several projected time series.

38  
39 354 Results indicate that uncertainty from parameter choice may become important, either in magnitude or variability  
40  
41 355 over time. It was also found a dependency between model structure complexity and parameter uncertainty.  
42  
43 356 Inspection of the discrepancies of projections shows a major contribution due to GCMs in Rhine and Ganges.  
44  
45 357 Interestingly, these results cannot be generalized as other researchers found an equivalent uncertainty introduced  
46  
47 358 by model structure. Overall, we conclude that relative discrepancies of impact rainfall-runoff models and its  
48  
49 359 influence on uncertainty in the parametrization (parameter uncertainty) are not negligible. This pattern was  
50  
51 360 observed in both regions varying in proportion according to period and RCP projection. This uncertainty might be  
52  
53 361 reduced by utilizing more sophisticated models that better capture input signals and able to react more accurately  
54  
55 362 to them; its general influence on global predictive model uncertainty should not be ignored.

56  
57  
58  
59  
60  
61  
62  
63  
64  
65

1 363 In the light of the results, It is advisable to consider different contributions of uncertainty when performing  
2  
3 364 projections. As it is shown in this study, parameter uncertainty may contribute to some extent to differences in  
4  
5 365 projected values.

6  
7 366

8  
9 367

10  
11 368 **Acknowledgments** The authors sincerely thank the Deutsche Forschungsgemeinschaft for funding this  
12  
13 369 work (BR 2238/5-2).

14  
15 370

16

17

18

19

20

21

22

23

24

25

26

27

28

29

30

31

32

33

34

35

36

37

38

39

40

41

42

43

44

45

46

47

48

49

50

51

52

53

54

55

56

57

58

59

60

61

62

63

64

65



## References

- Bárdossy, A., 2007. Calibration of hydrological model parameters for ungauged catchments. *Hydrol. Earth Syst. Sci. Discuss.* 11, 703–710.
- Bárdossy, A., Singh, S.K., 2008. Robust estimation of hydrological model parameters. *Hydrol. Earth Syst. Sci.* 12, 1273–1283.
- Barnett, V., 1976. The Ordering of Multivariate Data. *J. R. Stat. Soc. Ser. Gen.* 139, 318–355.  
doi:10.2307/2344839
- Bergström, S., 1995. The HBV model. 443–476.
- Boyle, D.P., Gupta, H.V., Sorooshian, S., Koren, V., Zhang, Z., Smith, M., 2001. Toward improved streamflow forecasts: value of semidistributed modeling. *Water Resour. Res.* 37, 2749–2759.  
doi:10.1029/2000WR000207
- Chen, J., Brissette, F.P., Poulin, A., Leconte, R., 2011. Overall uncertainty study of the hydrological impacts of climate change for a Canadian watershed. *Water Resour. Res.* 47, W12509.  
doi:10.1029/2011WR010602
- Donoho, D.L., Gasko, M., 1992. Breakdown Properties of Location Estimates Based on Halfspace Depth and Projected Outlyingness. *Ann. Stat.* 20, 1803–1827. doi:10.1214/aos/1176348890
- Exbrayat, J.-F., Buytaert, W., Timbe, E., Windhorst, D., Breuer, L., 2014. Addressing sources of uncertainty in runoff projections for a data scarce catchment in the Ecuadorian Andes. *Clim. Change* 125, 221–235.  
doi:10.1007/s10584-014-1160-x
- Fraiman, R., Liu, R.Y., Meloche, J., 1997. Multivariate Density Estimation by Probing Depth. *Lect. Notes-Monogr. Ser.* 31, 415–430.
- Götzinger, J., Bárdossy, A., 2008. Generic error model for calibration and uncertainty estimation of hydrological models. *Water Resour. Res.* 44, W00B07. doi:10.1029/2007WR006691
- Haddeland, I., Clark, D.B., Franssen, W., Ludwig, F., Voß, F., Arnell, N.W., Bertrand, N., Best, M., Folwell, S., Gerten, D., Gomes, S., Gosling, S.N., Hagemann, S., Hanasaki, N., Harding, R., Heinke, J., Kabat, P., Koirala, S., Oki, T., Polcher, J., Stacke, T., Viterbo, P., Weedon, G.P., Yeh, P., 2011. Multimodel Estimate of the Global Terrestrial Water Balance: Setup and First Results. *J. Hydrometeorol.* 12, 869–884. doi:10.1175/2011JHM1324.1
- Harding, B.L., Wood, A.W., Prairie, J.R., 2012. The implications of climate change scenario selection for future streamflow projection in the Upper Colorado River Basin. *Hydrol Earth Syst Sci* 16, 3989–4007.  
doi:10.5194/hess-16-3989-2012
- Hempel, S., Frieler, K., Warszawski, L., Schewe, J., Piontek, F., 2013. A trend-preserving bias correction – the ISI-MIP approach. *Earth Syst Dynam* 4, 219–236. doi:10.5194/esd-4-219-2013
- Hugg, J., Rafalin, E., Seyboth, K., Souvaine, D., 2006. An Experimental Study of Old and New Depth Measures, in: 2006 Proceedings of the Eighth Workshop on Algorithm Engineering and Experiments (ALENEX), Proceedings. Society for Industrial and Applied Mathematics, pp. 51–64.
- Hundecha Hirpa, Y., 2005. Regionalization of parameters of a conceptual rainfall runoff model.
- Hundecha, Y., Bárdossy, A., 2004. Modeling of the effect of land use changes on the runoff generation of a river basin through parameter regionalization of a watershed model. *J. Hydrol.* 292, 281–295.  
doi:10.1016/j.jhydrol.2004.01.002
- Jung, I.-W., Chang, H., 2011. Assessment of future runoff trends under multiple climate change scenarios in the Willamette River Basin, Oregon, USA. *Hydrol. Process.* 25, 258–277. doi:10.1002/hyp.7842
- Kavetski, D., Franks, S.W., Kuczera, G., 2003. Confronting Input Uncertainty in Environmental Modelling, in: Duan, Q., Gupta, H.V., Sorooshian, S., Rousseau, A.N., Turcotte, R. (Eds.), *Calibration of Watershed Models*. American Geophysical Union, pp. 49–68.
- Kirkpatrick, S., Gelatt, C.D., Vecchi, M.P., 1983. Optimization by Simulated Annealing. *Science* 220, 671–680.  
doi:10.1126/science.220.4598.671
- Lindström, G., Johansson, B., Persson, M., Gardelin, M., Bergström, S., 1997. Development and test of the distributed HBV-96 hydrological model. *J. Hydrol.* 201, 272–288. doi:10.1016/S0022-1694(97)00041-3
- Liu, R.Y., 1990. On a Notion of Data Depth Based on Random Simplices. *Ann. Stat.* 18, 405–414.  
doi:10.1214/aos/1176347507
- Liu, R.Y., Parelius, J.M., Singh, K., 1999. Multivariate analysis by data depth: descriptive statistics, graphics and inference, (with discussion and a rejoinder by Liu and Singh). *Ann. Stat.* 27, 783–858.  
doi:10.1214/aos/1018031260
- Miller, K., Ramaswami, S., Rouseeuw, P., Sellarès, J.A., Souvaine, D., Streinu, I., Struyf, A., 2003. Efficient computation of location depth contours by methods of computational geometry. *Stat. Comput.* 13, 153–162. doi:10.1023/A:1023208625954
- Moore, R., 1985. The probability-distributed principle and runoff production at point and basin scales. *Hydrol. Sci. J.* 30, 273–297.

- Nash, J.E., Sutcliffe, J.V., 1970. River flow forecasting through conceptual models part I — A discussion of principles. *J. Hydrol.* 10, 282–290. doi:10.1016/0022-1694(70)90255-6
- Oja, H., 1983. Descriptive statistics for multivariate distributions. *Stat. Probab. Lett.* 1, 327–332. doi:10.1016/0167-7152(83)90054-8
- Rousseeuw, P.J., Struyf, A., 1998. Computing location depth and regression depth in higher dimensions. *Stat. Comput.* 8, 193–203. doi:10.1023/A:1008945009397
- Schaeffli, B., Talamba, D.B., Musy, A., 2007. Quantifying hydrological modeling errors through a mixture of normal distributions. *J. Hydrol.* 332, 303–315. doi:10.1016/j.jhydrol.2006.07.005
- Singh, S.K., 2010. Robust parameter estimation in gauged and ungauged basins.
- Singh, V.P., Woolhiser, D.A., 2002. Mathematical modeling of watershed hydrology. *J. Hydrol. Eng.* 7, 270–292.
- Taylor KE, Stouffer RJ, Meehl GA (2012) An overview of CMIP5 and the experiment design. *Bull Amer Meteorol Soc* 93(4):485–498
- Teng, J., Vaze, J., Chiew, F.H.S., Wang, B., Perraud, J.-M., 2011. Estimating the Relative Uncertainties Sourced from GCMs and Hydrological Models in Modeling Climate Change Impact on Runoff. *J. Hydrometeorol.* 13, 122–139. doi:10.1175/JHM-D-11-058.1
- Tukey, J.W., 1975. Mathematics and the picturing of data. Presented at the Proceedings of the international congress of mathematicians, pp. 523–531.
- Uppala, S. M., KÅllberg, P. W., Simmons, A. J., Andrae, U., Bechtold, V. D. C., Fiorino, M., Gibson, J. K., Haseler, J., Hernandez, A., Kelly, G. A., Li, X., Onogi, K., Saarinen, S., Sokka, N., Allan, R. P., Andersson, E., Arpe, K., Balmaseda, M. A., Beljaars, A. C. M., Berg, L. V. D., Bidlot, J., Bormann, N., Caires, S., Chevallier, F., Dethof, A., Dragosavac, M., Fisher, M., Fuentes, M., Hagemann, S., Hólm, E., Hoskins, B. J., Isaksen, L., Janssen, P. A. E. M., Jenne, R., McNally, A. P., Mahfouf, J.-F., Morcrette, J.-J., Rayner, N. A., Saunders, R. W., Simon, P., Sterl, A., Trenberth, K. E., Untch, A., Vasiljevic, D., Viterbo, P. and Woollen, J. (2005), The ERA-40 re-analysis. *Q.J.R. Meteorol. Soc.*, 131: 2961–3012. doi:10.1256/qj.04.176
- Vardi, Y., Zhang, C.-H., 2000. The multivariate L1-median and associated data depth. *Proc. Natl. Acad. Sci.* 97, 1423–1426. doi:10.1073/pnas.97.4.1423
- Wagener, T., Boyle, D.P., Lees, M.J., Wheater, H.S., Gupta, H.V., Sorooshian, S., 2001. A framework for development and application of hydrological models. *Hydrol. Earth Syst. Sci. Discuss.* 5, 13–26.
- Weedon, G.P., Gomes, S., Viterbo, P., Shuttleworth, W.J., Blyth, E., Österle, H., Adam, J.C., Bellouin, N., Boucher, O., Best, M., 2011. Creation of the WATCH Forcing Data and Its Use to Assess Global and Regional Reference Crop Evaporation over Land during the Twentieth Century. *J. Hydrometeorol.* 12, 823–848. doi:10.1175/2011JHM1369.1
- Wilby, R.L., 2005. Uncertainty in water resource model parameters used for climate change impact assessment. *Hydrol. Process.* 19, 3201–3219. doi:10.1002/hyp.5819
- Wilby, R.L., Harris, I., 2006. A framework for assessing uncertainties in climate change impacts: Low-flow scenarios for the River Thames, UK. *Water Resour. Res.* 42, W02419. doi:10.1029/2005WR004065
- Zuo, Y., Serfling, R., 2000. General Notions of Statistical Depth Function. *Ann. Stat.* 28, 461–482.

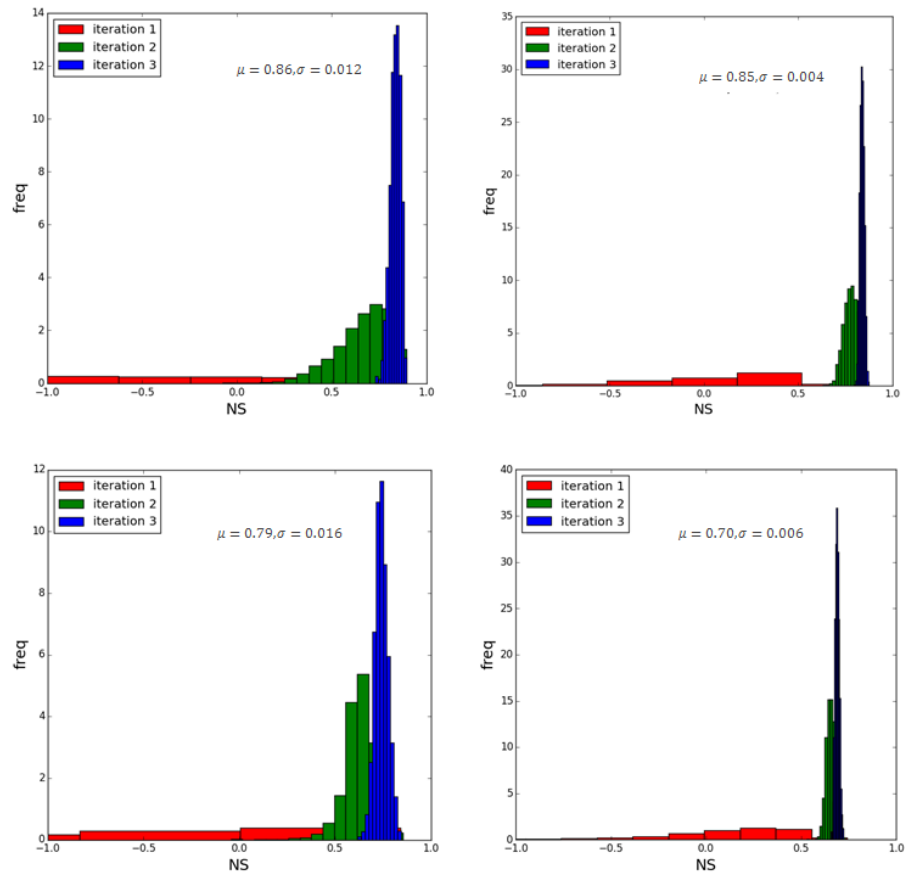


**Figure 1:** Histograms of the model performances (NSE) for the  $m = 5,000$  parameter sets showing the different iterations of ROPE for both basins and both models: Model HBV basin Rhine (top left), HBV Ganges (top right), HYMOD Rhine (bottom left) and HYMOD Ganges (bottom right).

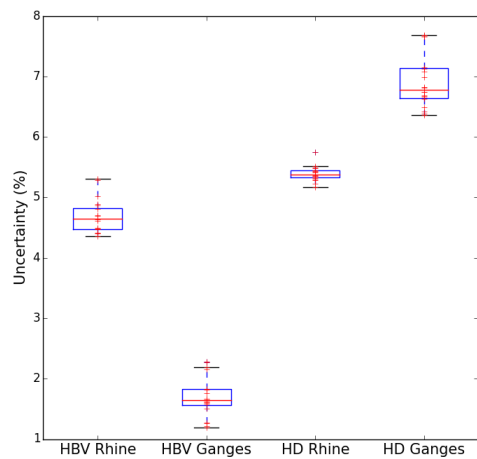


**Figure 2:** Parameter related uncertainty in discharge projections for the models HBV and HYMOD (HD) for the basins Rhine at Lobith and Ganges at Farakka. Time period considered 2006-2099.

**Table 1:** Statistics corresponding to the final iteration of ROPE algorithm with the selected 1,000 best performing sets for the two basins Rhine and Ganges and both models HBV and HYMOD

Basin		Min NS	Max NS	Mean	Std
Rhine	HBV	0.836	0.894	0.856	0.012
	HYMOD	0.770	0.845	0.790	0.016
Ganges	HBV	0.848	0.869	0.854	0.004
	HYMOD	0.690	0.723	0.701	0.006

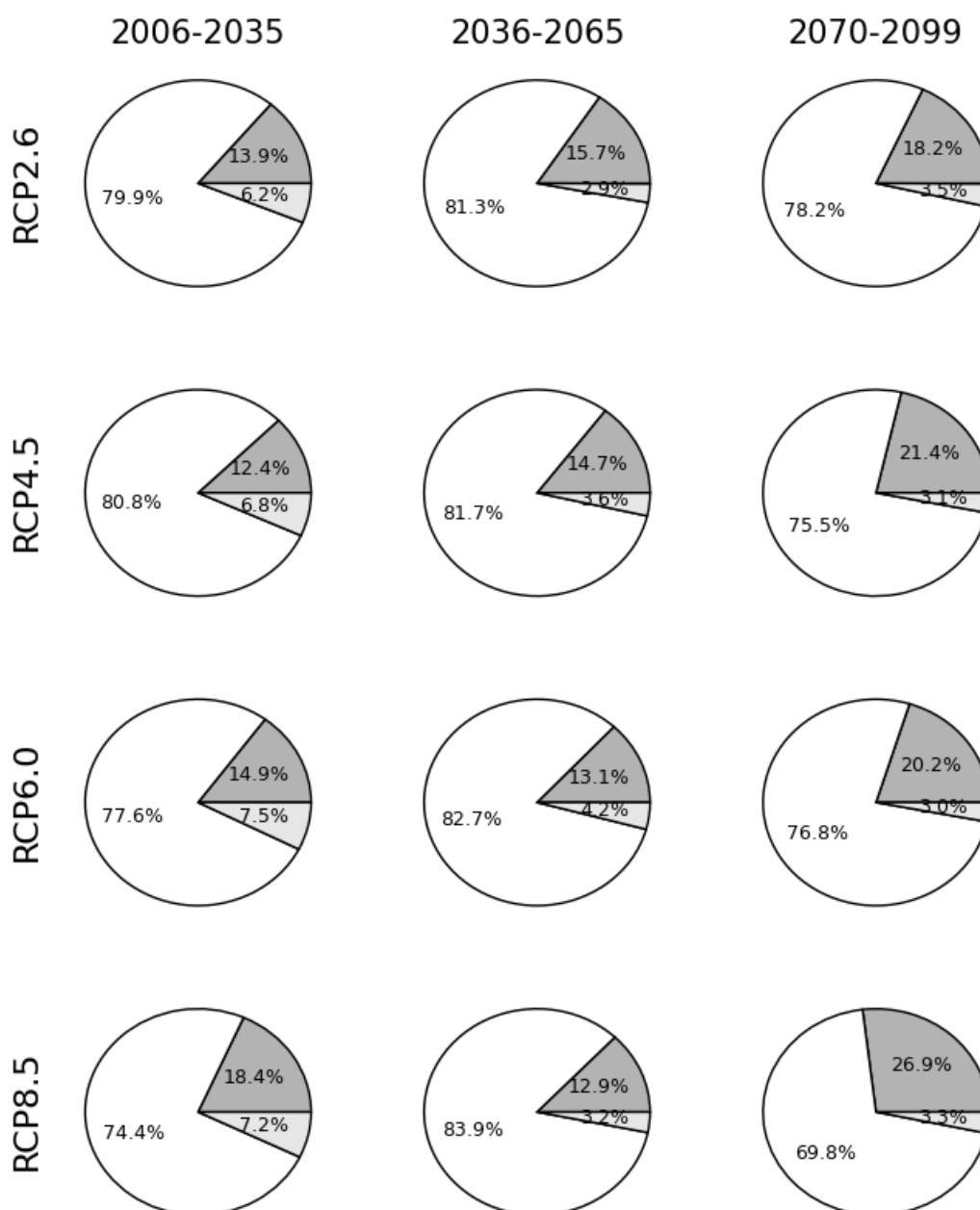


**Figure 3:** Contribution of GCM (white), rainfall-runoff model (grey) and parameter set (light grey) to the global model uncertainty. Basin Ganges at Farakka.

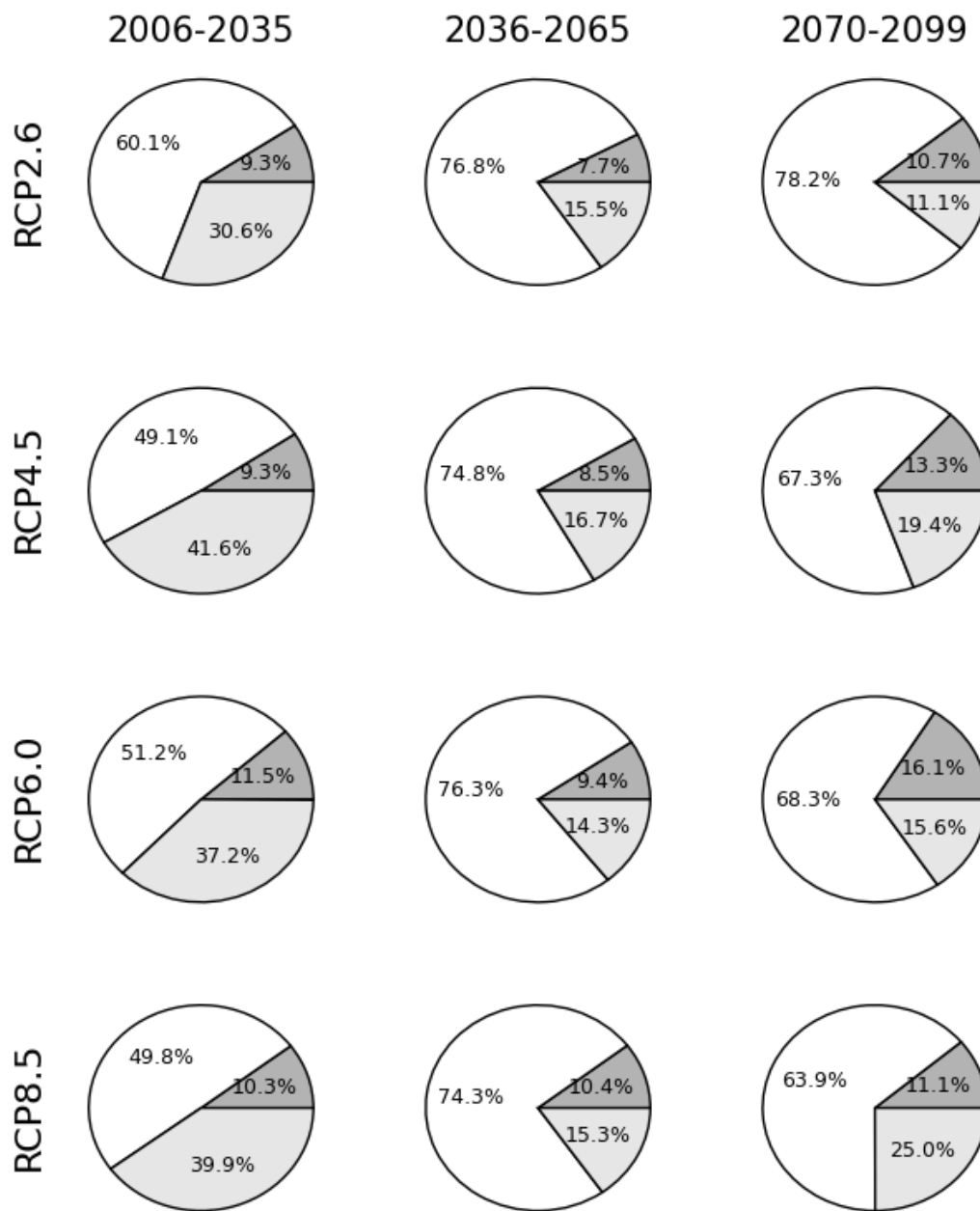


**Figure 4:** Contribution of GCM (white), rainfall-runoff model (grey) and parameter set (light grey) to the global model uncertainty. Basin Rhine at Lobith.

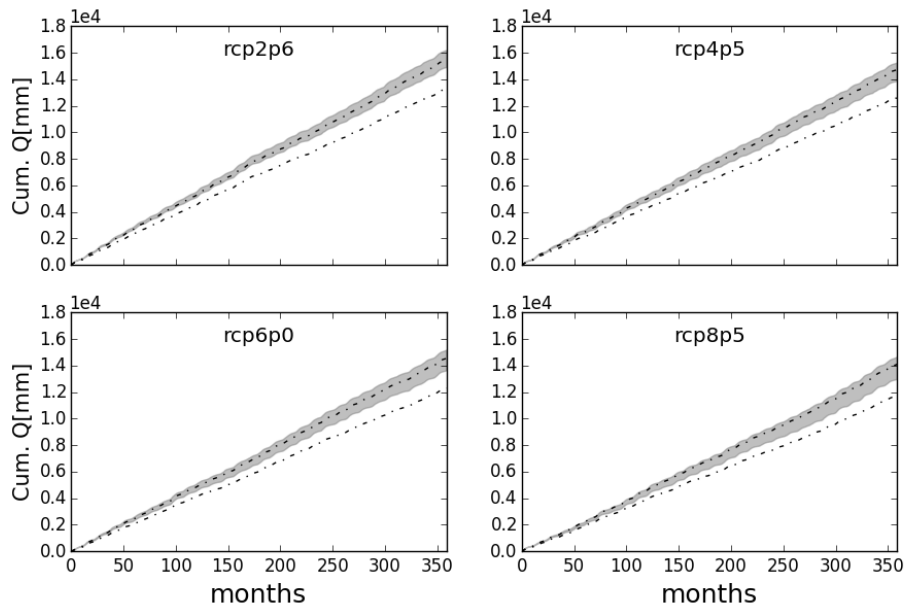


**Figure 5:** Projected discharge plots from the two impact models runs with data from GFDL-ESM2M and RCP2.6. Basin Rhine.